Multimode Oscillations in Two Coupled van der Pol Oscillators with Ninth-Power Nonlinear Characteristics

Mitsuhiro Yoneda†, Yasuteru Hosokawa‡, Yoshifumi Nishio† and Akio Ushida†

† Dept. of E. E. Eng., Tokushima University
Tokushima 770-8506, Japan
yoneda@ee.tokushima-u.ac.jp

‡ Dept. of Information Sci., Shikoku University
Tokushima 771-1192, Japan

1. Introduction

Coupled oscillators are good models to describe various nonlinear phenomena in the field of natural science and a number of excellent studies on such systems have been carried out. Datardina and Linkens have investigated two van der Pol oscillators with hard nonlinearities coupled by an inductor [1]. They have confirmed that nonresonant double-mode oscillations, namely simultaneous asynchronous oscillation of two periodic oscillations which could not occur for the case of third-power nonlinearity, were stably excited in the coupled systems. They have also confirmed that four different modes coexist for a range of parameter values; zero, two single-modes, and a double-mode. Yoshinaga and Kawakami have investigated a ring of van der Pol oscillators with hard nonlinearities and have confirmed interesting synchronization phenomena of double-mode oscillations [2].

In this study, we investigate multimode oscillations observed from two van der Pol oscillators with ninth-power nonlinear characteristics coupled by an inductor. By circuit experiments and computer calculations, we confirm that eight different modes coexist for a range of parameter values; zero, two in-phase single-modes, two anti-phase single-modes, and three different double-mode oscillations.

2. van der Pol Oscillator with Ninth-Power Nonlinear Characteristics

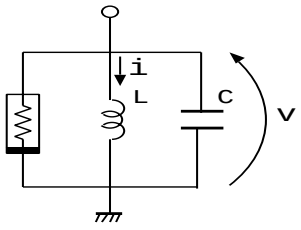

Figure 1: van der Pol oscillator.

Figure 1 shows van der Pol oscillator. We consider the case that the $v-i$ characteristics of the nonlinear resistor in the oscillator are represented by ninth-power nonlinear function. In order to realize the complicated nonlinear characteristics by real circuit, we approximate the ninth-power nonlinear function by the nine-segment piecewise-liner function as shown in Fig. 2. The function is described by using 4 parameters (B_0, B_1, B_2, B_3) corresponding to the breakpoints and 5 parameters $(G_0, G_1, G_2, G_3, G_4)$ corresponding to the resistances as follows.

$$i(v) = \begin{cases} G_4 v + B_3(G_3+G_4) - B_2(G_2+G_3) \\ \quad +B_1(G_1+G_2) - B_0(G_0+G_1) \\ \qquad\qquad \cdots (v < -B_3) \\ -G_3 v - B_2(G_2+G_3) + B_1(G_1+G_2) \\ \quad -B_0(G_0+G_1) \qquad \cdots (-B_3 < v < -B_2) \\ G_2 v + B_1(G_1+G_2) - B_0(G_0+G_1) \\ \qquad\qquad \cdots (-B_2 < v < -B_1) \\ -G_1 v - B_0(G_0+G_1) \cdots (-B_1 < v < -B_0) \\ G_0 v \qquad\qquad \cdots (|v| < B_0) \\ -G_1 v + B_0(G_0+G_1) \qquad \cdots (B_0 < v < B_1) \\ G_2 v - B_1(G_1+G_2) + B_0(G_0+G_1) \\ \qquad\qquad \cdots (B_1 < v < B_2) \\ -G_3 v + B_2(G_2+G_3) - B_1(G_1+G_2) \\ \quad +B_0(G_0+G_1) \qquad \cdots (B_2 < v < B_3) \\ G_4 v - B_3(G_3+G_4) + B_2(G_2+G_3) \\ \quad -B_1(G_1+G_2) + B_0(G_0+G_1) \ \cdots (B_3 < v) \end{cases} \tag{1}$$

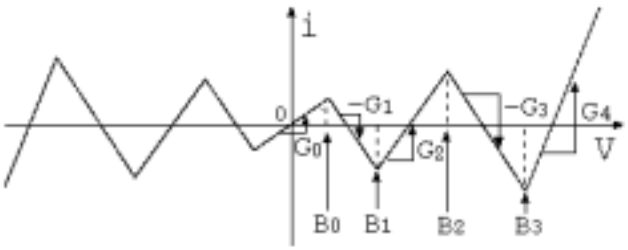

Figure 2: Approximation of the ninth-power $v-i$ characteristics of nonlinear negative resistor.

The equation governing the circuit in Fig. 1 is de-

scribed as follows:

$$\begin{aligned} L\frac{di}{dt} &= v \\ C\frac{dv}{dt} &= -i - i(v) \end{aligned} \tag{2}$$

By changing the variable and the parameters,

$$\begin{aligned} &i = \sqrt{\frac{C}{L}}\frac{y}{a},\ v = B_0 x,\ t = \sqrt{LC}\tau,\ \text{“}\cdot\text{”} = \frac{d}{d\tau}, \\ &\varepsilon = a\sqrt{\frac{L}{C}},\ \beta_1 = \frac{B_1}{B_0},\ \beta_2 = \frac{B_2}{B_0},\ \beta_3 = \frac{B_3}{B_0}, \\ &\gamma_0 = B_0 G_0,\ \gamma_1 = B_0 G_1,\ \gamma_2 = B_0 G_2, \\ &\gamma_3 = B_0 G_3,\ \gamma_4 = B_0 G_4, \end{aligned} \tag{3}$$

(2) is normalized as

$$\begin{aligned} \dot{y} &= x \\ \dot{x} &= -y - \varepsilon f(x) \end{aligned} \tag{4}$$

where the function $f(x)$ corresponds to $i(v)$ and is represented as follows.

$$f(x) = \begin{cases} \gamma_4 x + \beta_3\gamma_4 + (\beta_3 - \beta_2)\gamma_3 - (\beta_2 - \beta_1)\gamma_2 \\ \quad +(\beta_1 - 1)\gamma_1 - \gamma_0 & \cdots (x < -\beta_3) \\ -\gamma_3 x - \beta_2\gamma_3 - (\beta_2 - \beta_1)\gamma_2 \\ \quad +(\beta_1 - 1)\gamma_1 - \gamma_0 & \cdots (-\beta_3 < x < -\beta_2) \\ \gamma_2 x + \beta_1\gamma_2 + (\beta_1 - 1)\gamma_1 - \gamma_0 & \\ & \cdots (-\beta_2 < x < -\beta_1) \\ -\gamma_1 x - (\gamma_0 + \gamma_1) & \cdots (-\beta_1 < x < -1) \\ \gamma_0 x & \cdots (|x| < 1) \\ -\gamma_1 x + (\gamma_0 + \gamma_1) & \cdots (1 < x < \beta_1) \\ \gamma_2 x - \beta_1\gamma_2 - (\beta_1 - 1)\gamma_1 + \gamma_0 & \\ & \cdots (\beta_1 < x < \beta_2) \\ -\gamma_3 x + \beta_2\gamma_3 + (\beta_2 - \beta_1)\gamma_2 \\ \quad -(\beta_1 - 1)\gamma_1 + \gamma_0 & \cdots (\beta_2 < x < \beta_3) \\ \gamma_4 x - \beta_3\gamma_4 - (\beta_3 - \beta_2)\gamma_3 + (\beta_2 - \beta_1)\gamma_2 \\ \quad -(\beta_1 - 1)\gamma_1 + \gamma_0 & \cdots (\beta_3 < x) \end{cases} \tag{5}$$

By circuit experiments and computer calculations, we confirmed that this circuit have two sizes of oscillations and that the origin is stable for the same parameter values. Figure 3 shows two sizes of oscillations observed from the circuit. Figure 3(a) shows the small oscillation. In this case, the solution uses the inside negative resistance regions between $\pm B_0$ and $\pm B_1$, namely the solution does not reach the regions beyond the breakpoints $\pm B_2$. Figure 3(b) shows the large oscillation. In this case, the solution uses the outside negative resistance regions between $\pm B_2$ and $\pm B_3$ in Fig. 2.

3. Two Coupled Oscillators

The main object of this paper is to investigate two van der Pol oscillators with ninth-power hard nonlinearities coupled by a inductor. The coupled model is shown in Fig. 4.

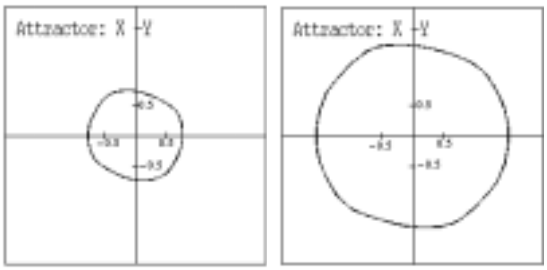

(a) (b)

Figure 3: Two different sizes of oscillations obtained by computer calculations. Horizontal axis is x and vertical axis is y. $\alpha = 0.05$, $\beta_1 = 2.3$, $\beta_2 = 4.18$, $\beta_3 = 6.27$, $\gamma_0 = 0.17$, $\gamma_1 = 0.35$, $\gamma_2 = 0.34$, $\gamma_3 = 0.37$, $\gamma_4 = 0.60$, $\varepsilon = 0.3$. (a) Small oscillation. (b) Large oscillation.

Figure 5 shows the circuit realization of the negative resistor with the nine-segment piecewise-linear $v-i$ characteristics. Figure 6 shows the measured $v - i$ characteristics of the negative resistor.

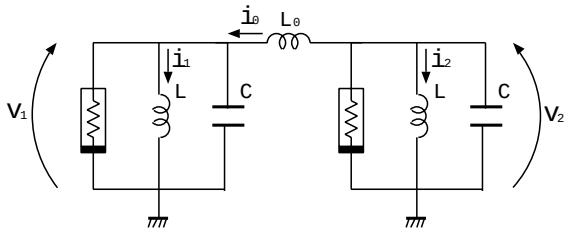

Figure 4: Two van der Pol oscillators coupled by an inductor.

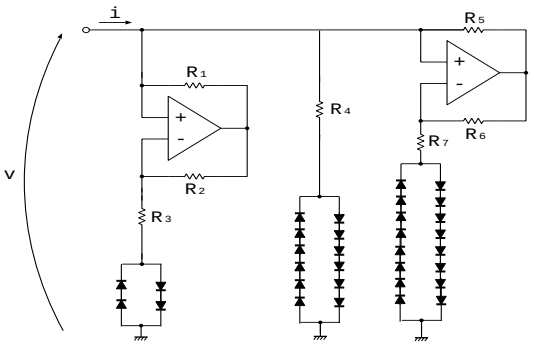

Figure 5: Circuit realization of the negative resistor with the nine-segment piecewise-linear $v - i$ characteristics. R_1 = R_2=47kΩ, R_3=1.2kΩ, R_4=6.2kΩ, R_5 = R_6=820Ω, and R_7=1.2kΩ.

The equations governing the circuit in Fig. 4 are given

Figure 6: Measured $v - i$ characteristics of the negative resistor.

as follows:

$$\begin{aligned} \dot{y_1} &= x_1 \\ \dot{x_1} &= -y_1 + \alpha(y_2 - y_1) - \varepsilon f(x) \\ \dot{y_2} &= x_2 \\ \dot{x_2} &= -y_2 + \alpha(y_1 - y_2) - \varepsilon f(x) \end{aligned} \tag{6}$$

where $\alpha = L/L_0$ is a new parameter corresponding to the coupling.

In the following circuit experiments, the circuit parameters are fixed as L = 200mH, L_0 = 1.15H, and C = 100nF. While for the computer calculations, the parameter values are as $\alpha = 0.05$, $\beta_1 = 2.3$, $\beta_2 = 3.8$, $\beta_3 = 5.75$, $\gamma_0 = 0.052$, $\gamma_1 = 0.087$, $\gamma_2 = 0.087$, $\gamma_3 = 0.108$, $\gamma_4 = 1.86$, $\varepsilon = 0.3$. Further, (6) is integrated by using the Runge-Kutta method with step size $h = 0.005$.

From the coupled circuit in Fig. 4, we confirmed that eight different oscillation modes coexist; zero, two in-phase single-modes, two anti-phase single-modes and three double-modes. Zero means that both of two oscillators are not excited. This state is always stable and relatively small initial values are attracted to this state. In the following we do not show any figures of this state, because it is trivial. In-phase single-mode means that the two oscillators are synchronized at the in-phase. Two different sizes of the in-phase single-mode oscillations are shown in Figs. 7(a) and 8(a). Anti-phase single-mode means that the two oscillators are synchronized at the anti-phase. Two different sizes of the anti-phase single-mode oscillations are shown in Figs. 7(b) and 8(b).

4. Double-mode Oscillation

Double-mode means that above two single-mode oscillations, namely in-phase and anti-phase single-modes, are simultaneously excited. We have found three different types of double-mode oscillations from our circuit model. The circuit experimental results and the corresponding computer calculated results are shown in Figs. 9 and 10, respectively. We can characterize the three double-mode oscillations as follows. In Figs. 9(1) and 10(1), the solution moves from zero to small oscillation alternately. In other words, the double-mode oscillation consists of zero and small oscillation. In Figs. 9(2)

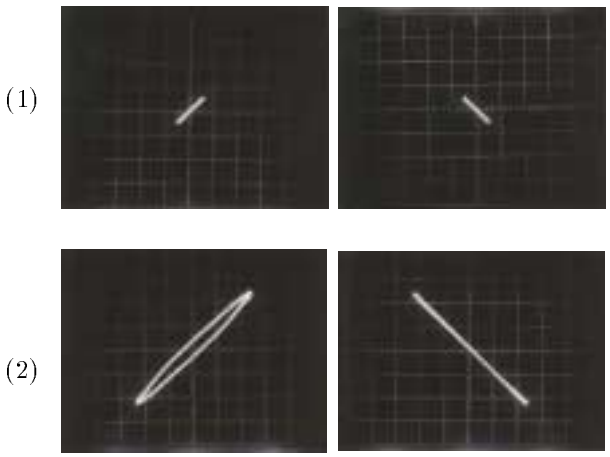

Figure 7: Circuit experimental results of single-mode oscillations. (a) In-phase single-mode. (b) Anti-phase single-mode. (1) Small oscillation. (2) Large oscillation. Horizontal axis is v_1 [2V/div.] and vertical axis is v_2 [2V/div.].

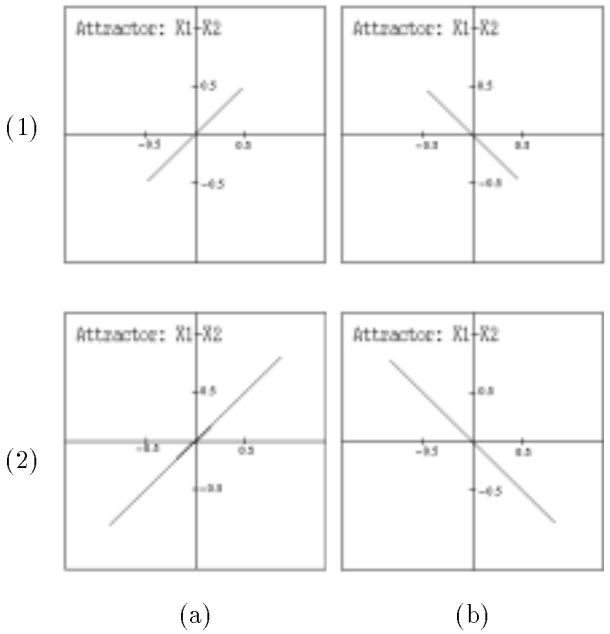

Figure 8: Computer calculated results of single-mode oscillations. (a) In-phase single-mode. (b) Anti-phase single-mode. (1) Small oscillation. (2) Large oscillation.

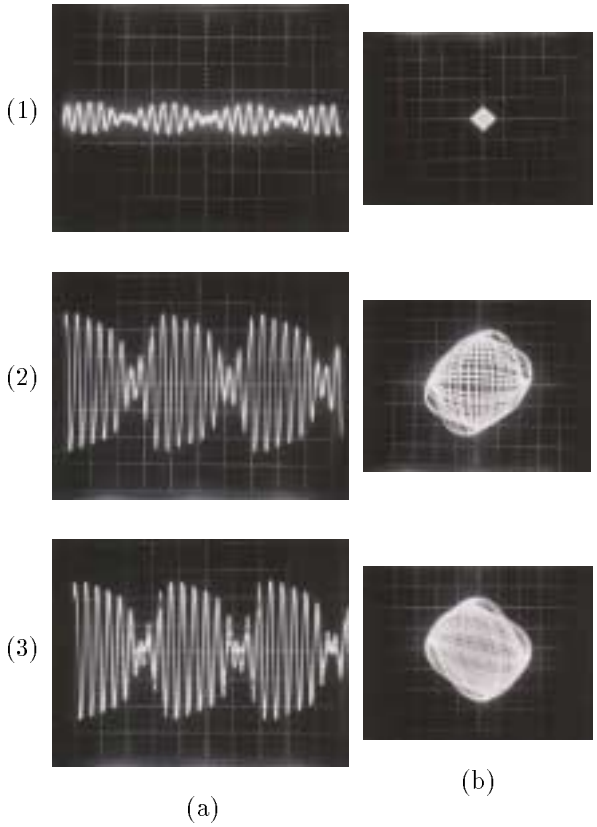

Figure 9: Circuit experimental results of double-mode oscillations. (a) Time waveforms. Horizontal axis is t [2ms/div.] and vertical axis is v_1 [5V/div.]. (b) Attractors. Horizontal axis is v_1 [2V/div.] and vertical axis is v_2 [2v/div.]. (1) Double-mode oscillation consisting of zero and small oscillation. (2) Double-mode oscillation consisting of small and large oscillations. (3) Double-mode oscillation consisting of zero and large oscillation.

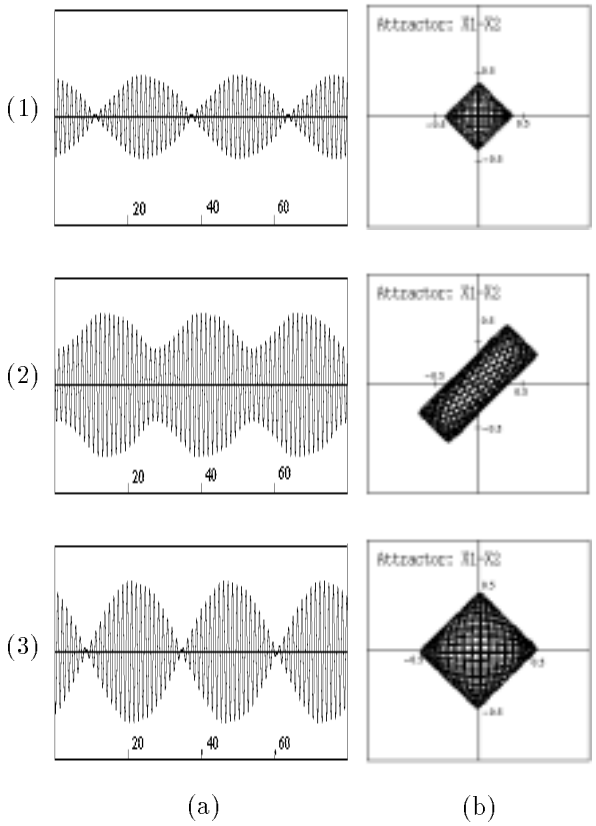

Figure 10: Computer calculated results of double-mode oscillations. (a) Time waveforms. Horizontal axis is τ and vertical axis is x_1. (b) Attractors. Horizontal axis is x_1 and vertical axis is x_2. (1) Double-mode oscillation consisting of zero and small oscillation. (2) Double-mode oscillation consisting of small and large oscillations. (3) Double-mode oscillation consisting of zero and large oscillation.

and 10(2), the solution moves from small oscillation to large oscillation alternately. In other words, the double-mode oscillation consists of small and large oscillations. Finally, in Figs. 9(3) and 10(3), the solution moves from zero to large oscillation alternately. In other words, the double-mode oscillation consists of zero and large oscillations. Namely, we can characterize the double-mode oscillations by using the stable states included in the oscillations. This would be an interesting approach to analyze multimode oscillations observed from complex nonlinear circuits.

5. Concluding Remarks

In this study, we have investigated multimode oscillations observed from two van der Pol oscillators with ninth-power nonlinear characteristics coupled by an inductor. By both circuit experiments and computer calculations, we confirmed that eight different oscillation modes coexist for a range of parameter values; zero, two in-phase single-modes, two anti-phase single-modes, and three double-modes.

We consider that there remain some interesting problems. In the present circuit model, we could not find the multimode oscillation consisting of three possible stable states; zero, small oscillation and large oscillation. The oscillation could be a triple-mode oscillation. Further, theoretical analysis should be carried out to investigate the stability of the various modes of oscillations.

References

[1] S. P. Datardina and D. A. Linkens, "Multimode oscillations in mutually coupled van der pol type oscillators with fifth-power nonlinear characteristics," *IEEE Trans. Circuits Syst.*, vol. 25, no. 5, pp. 308-315, May 1978.

[2] T. Yoshinaga and H. Kawakami, "Synchronized quasi-periodic oscillations in a ring of coupled oscillators with hard characteristics," *Trans. IEICE*, vol. J75-A, no. 12, pp. 1811–1818, Dec. 1992.